Influence of ultrasonic agitation on Co-γ-Al_2O_3 nano-electrocomposite coating

Menini, Richard; Vignola, Éric

Publisher's version / Version de l'éditeur:

Electrochimica Acta, 2006-01-01

Influence of Ultrasonic Agitation on Co-γ-Al_2O_3 Nano-Electrocomposite Coating Process

Richard Menini[1] and Éric Vignola[2]

National Research Council Canada, Industrial Materials Institute,

75 de Mortagne Blvd., Boucherville (QC), J4B 6Y4, Canada

[1]Corresponding author. Now at: Pavillon de recherche sur le givrage, Université du Québec à Chicoutimi, 555 Bd. de l'Université, Chicoutimi (QC), G7H 2B1, Canada. rmenini@uqac.ca

[2]Now at: Nova Chemicals Corporation, 2928 16 Street N.E., Calgary (AB), T2E 7K7, Canada. vignole@novachem.com

Abstract

Incorporation of a cationic surfactant, cetyltrimethylammonium chloride (CTAC), and use of ultrasonic agitation during electroplating of Co-γ-Al_2O_3 composite coatings resulted in high particle inclusion percentage with embedded alumina clusters being 2.5 to 3.0 times smaller than those obtained with conventional plating or when ultrasonic agitation was used only before plating. Alumina particles with high zeta potentials were obtained when CTAC was added to the plating bath and resulted in particles inclusion percentages 10 to 20 times higher than when a surfactant-free electrolyte was used. Ultrasonic agitation during electrodeposition acted as an effective alumina cluster refiner. Although ultrasonic agitation resulted in better particle dispersion for the Co-γ-Al_2O_3 system, no real improvement in term of hardness was observed compared to the same system plated without ultrasounds. Nonetheless, the positive dual effect of cationic surfactant addition and ultrasonic agitation was clearly demonstrated and can be applied to other types of electrocomposite bath compositions and therefore to other types of coating applications.

Keywords:

Electrocomposite coating, nanocomposite, ultrasonic agitation, zeta potential, turbidimetry, hardness, cobalt electroplating, alumina.

Introduction

Electrocomposite coatings (ECC) have drawn much attention over the last decade where many groups focused not only on wear resistant and hard coatings [1-6], but also recently on new applications such as electrocatalysis, photoactive coatings and energy storage [7]. By using a variety of combinations in terms of metal/alloy matrices and inert particles, as well as being a non-line-of-sight coating technique, the electrodeposition of composite coatings represents an attractive and low cost alternative technology for a variety of industrial applications. Many tunable parameters were studied in the literature in order to improve the targeted characteristics of a given coating. High particle inclusion percentage is often, but not always, linked to specific property enhancement. The main variables associated to particle inclusion percentage are current density (DC or pulse), particle surface chemistry, geometry, solution composition, hydrodynamics as well as particle surface interaction with plating bath components. Many interesting reviews can be found in the literature on the influence of these different parameters on coating properties and structures [7-9].

All types of particles, regardless of their size and shape, are superficially charged once added into an aqueous media, and that charge will have a preponderant effect on particle entrapment probability within the coating. The co-deposition mechanisms are well described in the literature and the work from Celis' group in Belgium represents the most reliable studies on the topic [10, 11]. This group showed that inert particles immersed in strong electrolytes will charge and/or hydrate up to a certain extent depending on their

surface composition. Following its ionic cloud formation, convection and diffusion steps, the particle contacts the cathode and then becomes adsorbed on its surface. Simultaneously the metallic cations surrounding the particle are being electrochemically reduced. This overall process is also referred as the "perfect sink conditions". Although the convection and diffusion steps represent the key steps in bringing the ceramic particles at an acceptable rate and velocity towards the cathode to produce a coating with a significant amount of co-deposited particles, the nature and overall charge of the particles are also very important, even for non-Brownian particles. The Celis group showed that the perfect sink conditions were not always respected. This is particularly true when very strong electrolytes are used (as it is the case in electroplating processes) or when highly hydrophilic particles such as quartz and most oxides are used. Many authors try to overcome such difficulties by using different approaches: by adsorbing monovalent cations (Tl^+, Rb^+ or Cs^+) on the particle surface [12, 13], by removing the surface oxide layer [14] or by adding surfactants into various plating formulations [2, 8, 15-19]. From the latter, addition of a cationic surfactant usually exhibits highest particle inclusion yields.

An additional difficulty arises when nanoparticles are being co-deposited, since these have the tendency to agglomerate in solution resulting in the entrapment of clusters instead of individual particles [20]. Two different strategies can be exploited to achieve dispersion: by using surfactants [15-19] or by the simple effect of the spinning of a rotating cylinder electrode (RCE) used for kinetics studies [21]. Few groups have attempted to disperse nanoparticles using ultrasonic agitation. To our knowledge, the first

authors to describe such a process for ECC coating were Petit *et al.* [22] who, in 1977, dispersed ThO_2 particles that were subsequently co-deposited with nickel. More recently, Lee *et al.* [23] dispersed diamond nanoparticles in water under sonication before being codeposited in a sulfamate nickel plating bath. Steinbach and Ferkel [24] and Erler *et al.* [20] also used ultrasonic treatment for dispersing alumina nanoparticles during nickel electroplating experiments. Since particle charge is inversely proportional to its radius and influenced by surfactant adsorption, it is very important to study both these variables. None of the aforementioned groups who used ultrasonic agitation as a method of particle dispersion considered the dual effect of organic surfactant addition and ultrasonic agitation upon particle dispersion. In the present study, both the influence of ultrasonic agitation and cationic surfactant addition on particle charge inside the plating bath and its dispersion within an electrocoating were studied for the Co-γ–Al_2O_3 system.

Experimental

Electroplating experiments

The Co-γ-Al_2O_3 coatings were electroplated on stainless steel 304 substrates, pre-treated according to the following procedure: alkaline medium (Supersoak^{TM}) cleaning step for 5 minutes at 65°C, water rinse, 2 minutes of pickling in H_2SO_4 10 % at room temperature and a final rinsing step in water. The plating solution was composed of $CoSO_4.7H_2O$ at 550 $g.l^{-1}$, $CoCl_2.6H_2O$ at 30 $g.l^{-1}$ and H_3BO_3 at 40 $g.l^{-1}$. Solution pH was maintained at 4.0 while the plating temperature was comprised between 35°C and 40°C. The plating current was 38 $mA.cm^{-2}$ (or 35 ASF). The γ-alumina particles were purchased from NanoTek. The spherical particles had a mean average diameter comprised between 27 and 56 nm with a surface area of 60 $m^2.g^{-1}$ (BET). The two cationic surfactants used for the experiments were ammonium salts: cetyltrimethylammonium chloride (CTAC) and tetrabutylammonium chloride (TBAC). Two different concentrations were used: low concentration (CTAC-L and TBAC-L) corresponding to 1.25 mmole per gram of alumina and high concentration (CTAC-H and TBAC-H) corresponding to 5.00 mmole per gram of alumina. The schematic representation of the electroplating set-up is shown in Fig. 1. As indicated in this figure, the ultrasonic transducer (f = 80 kHz and 300 W) was glued inside a titanium casing that was then placed at the bottom of a water filled polypropylene (PP) tank. Electroplating experiments were performed in a 500 ml Pyrex beaker placed in the PP tank. A cobalt anode was put inside a PP woven bag. The coating thickness was chosen at 50 µm. For all the experiments described in the results and discussion sections,

only the Al_2O_3 concentration, the hydrodynamic conditions (No UA, UA only 15 minutes prior (UAP) and UA 15 minutes prior and during the experiments (UAD)) as well as the type and concentration of the cationic surfactant were varied.

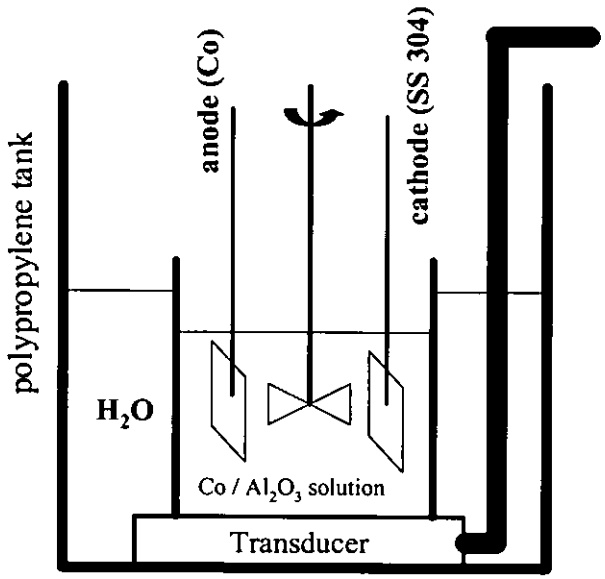

Fig. 1 – Schematic representation of the electroplating set-up.

Particle analysis

Zeta potential and particle size measurements were performed using a Malvern 3000 HSA ZetaSizer instrument. The powder concentration was chosen at 1 $g.l^{-1}$, the measurements were done following 15 minutes of UA and the elapsed period of time between the end of UA and the beginning of the velocity/size samplings was one minute. Turbidimetric data was acquired through a homemade apparatus using a low power laser diode (1 mW at 630 nm) and a silicon pin detector (PDA55) from ThorLabs Inc., see Fig. 2. Prior to each measurement, the colloidal solution was placed in a small quartz cuvette (1 x 1 x 5 cm)

and was either mechanically stirred by hand (No UA) or ultrasonicated (UAP) during 15 minutes. The cuvette was then positioned inside its holder with no further agitation and the power of the transmitted beam was recorded versus time. All measurements were recorded at ambient conditions in a cobalt plating solution diluted two times in water. This lower concentration was necessary in order not to compromise laser transmittance through the cuvette. It must be pointed out that for the turbidimetry assessment; the laser beam crossed the liquid suspension at 75 % of its height to minimize the time of the experiment. On the other hand and due to apparatus constraints, zeta potential measurements were performed at 20 % of liquid suspension height.

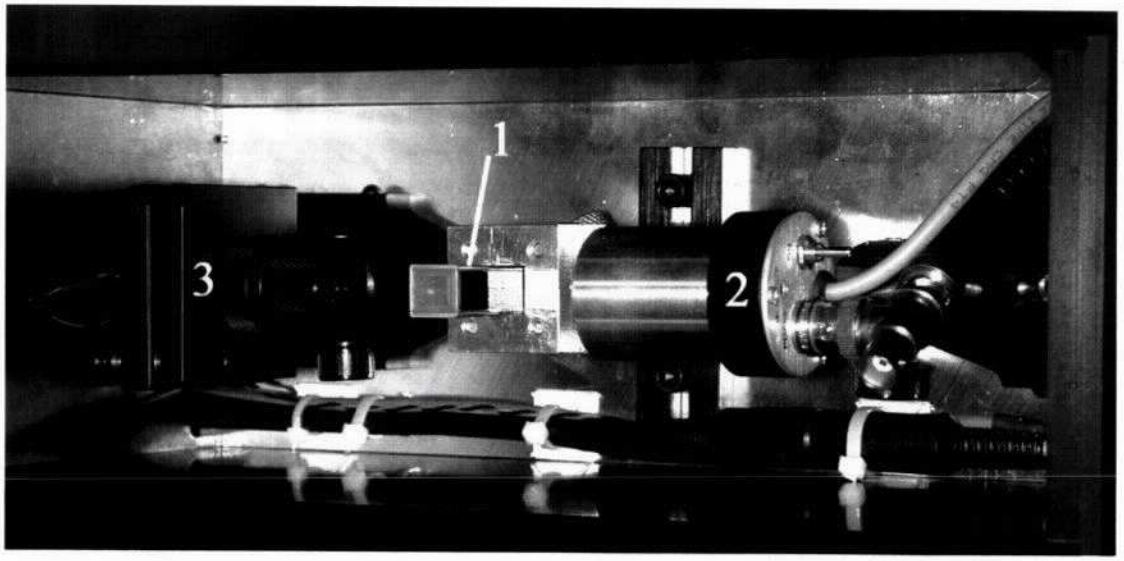

Fig. 2 – Top view of the apparatus for turbidimetric measurements.

(1) Quartz cuvette, (2) detector and (3) laser source.

Coating analysis

Polished cross-sectioned samples mounted in epoxy resin where observed using a Hitachi S-4700 scanning electron microscope (SEM) operating at 15 kV and at two different magnifications (5000 and 10000 times). Deposited cobalt and aluminum contents were determined using an Electron Dispersive Spectrometry (EDX) probe fitted within the S-4700 SEM. Coating hardness were determined using the Knoop method for an applied load of 100 g. For each plating condition, two samples were produced and ten hardness measurements were performed on each of them in order to obtain an averaged value.

Results and Discussion

Particle Characterization

The zeta potential measurements, see Fig. 3, were performed with and without ultrasonic agitation and surfactant addition. In the light of these results, it is clearly demonstrated that ultrasonic agitation had a strong influence on particle charge. Independently of the presence of surfactant, its hydrophobic chain length (CTAC or TBAC) or its concentration (Low or High), γ-Al_2O_3 particles gained on average 15.2 mV $\pm$ 3.1 mV on their zeta potential. Additionally, it must be noted that without UAP, the zeta potentials were negative when no surfactant or TBAC was added to the solution. On the other hand, all zeta potentials were positive when ultrasonic agitation was used. The highest zeta

potential values were found when CTAC was present in the electrolyte: 24.1 mV and 31 mV for CTAC-L and CTAC-H respectively. On the other hand, the presence of TBAC molecules did not charge the γ-Al_2O_3 particle positively due to what seems to be a lack of significant surfactant adsorption.

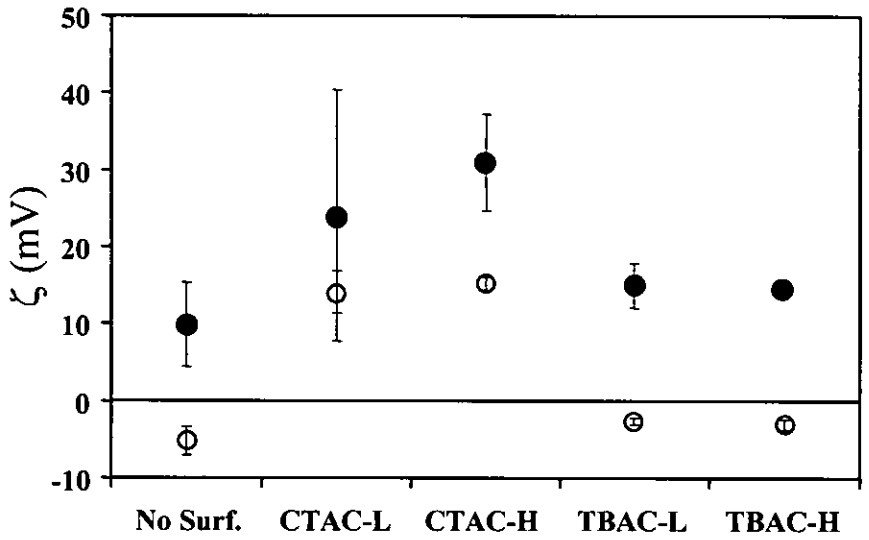

Fig. 3 – Zeta potential of γ-Al_2O_3 particles (C = 1 g.l^{-1}) in cobalt plating bath vs. surfactant type and concentration. (○) without (No UA) and (●) with ultrasonic agitation (UAP).

Particle (or cluster) size assessments during zeta potential measurements were conducted and the corresponding data are presented in Table 1. The particle size radii when TBAC-L and TBAC-H were used are not indicated in the table. In this particular case, no measurement was possible since the particles agglomerated and sedimentated too quickly when the solutions were not sonicated. For each chemical solution, ultrasonic agitation decreases particle cluster size. To summarize, ultrasonic agitation prior to measurement (UAP) increases particle zeta potential together with being a particle dispersant. On the

other hand, while it enhances zeta potentials, cationic surfactant CTAC do not act as an effective γ-Al_2O_3 particle dispersant in these highly conductive plating bath formulations. In fact and within the experimental error, all the clusters have the same size after ultrasonic agitation.

Table 1 – Particle cluster radius versus type of bath an agitation mode

	Particle cluster radius (μm)		
	No surfactant	CTAC-L	CTAC-H
No UA	5 to 10	20 to 30	20 to 30
UA	3	3 to 5	3 to 4

In order to evaluate the zeta potential, the electrophoretic mobility μ was calculated according to equation (1) where $\vec{v}$ is the particle velocity and $\vec{E}$ is the electrical field. The zeta potential (ξ) can be evaluated, see equation (2), knowing the solution viscosity (η) as well as the vacuum and solution permittivity constants, ε_0 and ε_r respectively. It must be pointed out that the electrophoretic mobility is directly proportional to the particle charge, q, and inversely proportional to its radius, r, as described in the Stoke equation (3). Therefore, as the particle radius increases, its zeta potential should decrease. The Stoke equation, thus confirms the experimental results where in the case of the surfactant-free system and in the cases of both low and high CTAC addition, low particle radius (see Table 1) corresponds to higher zeta potential values, see Fig. 3. Although particle radii were not determined for TBAC addition, the same trend was probably occurring. In the case of non-sonicated solutions, it is important to note that CTAC

addition at low or high concentration resulted in substantial increase (around 20 mV) in zeta potential values while in the case of TBAC addition this increase was marginal (around 2.5 mV). All the above increase of zeta potentials were occurring in spite of being in presence of high cluster radius when the CTAC was added (see Table 1). The CTAC molecules have a strong affinity to γ-Al_2O_3 surface [25] and are able to increase zeta potential even for high cluster radii. The combined effect of sonicated solution and CTAC addition gave highest zeta potential measured values together with being in the presence of low cluster size.

$$\mu = \frac{\vec{v}}{\vec{E}} \tag{1}$$

$$\xi = \frac{\eta}{\varepsilon_r \varepsilon_0} \mu \tag{2}$$

$$\mu = \frac{q}{6\pi\eta r} \tag{3}$$

Since ultrasonic agitation acts as a particle dispersant, turbidimetric measurements were performed at different alumina concentration in order to confirm and study in depth these observations. Two examples of diode potential vs. time type turbidimetry curves are shown in Fig. 4. In this figure, the destabilization time, t_d, is described as the time when the slope of the curve $U = f(t)$ is superior to 0. This value is determined by the derivative dU / dt. The k_{fast} value corresponds to the steepest slope for a given $U = f(t)$ curve.

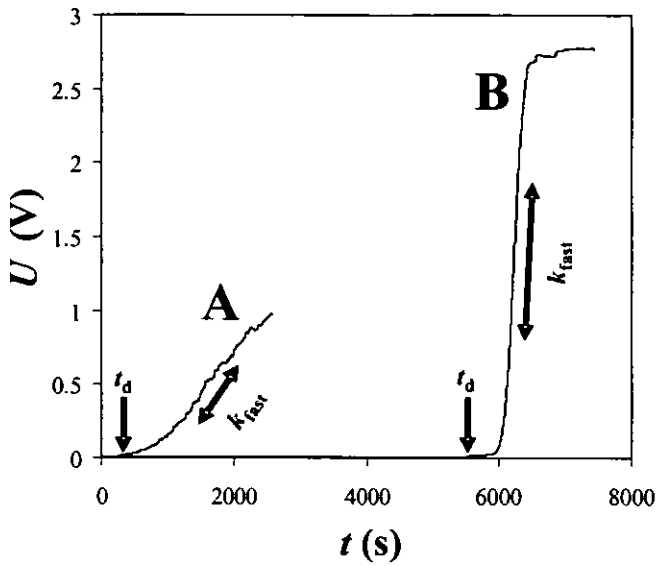

Fig. 4 – Turbidimetric measurements: diode potential vs. time at 25 g.l^{-1} γ-Al_2O_3 concentration and no surfactant. Without (No UA) (A) and with ultrasonic agitation prior to measurement (UAP) (B).

Figures 5 and 6 show the different t_d and k_{fast} values plotted versus the concentration of alumina particles (1, 5, 10, 25, 50 and 100 g.l^{-1}) in the simulated cobalt plating bath (no added surfactant) with and without UAP. As far as the t_d values were concerned, it is quite obvious that for concentration of alumina $\geq$ 25 g.l^{-1} and after UAP, the solution stayed turbid (stable) during longer periods compare to the solutions that did not undergo UAP. In fact, at C = 100 g.l^{-1}, the t_d value was 90000 s when UAP was used (point not indicated in the figure). By using UAP, the alumina cluster size is reduced and is less widespread, see Table 1, thus, the beginning of the settling process is appearing at longer periods compare to the case of large cluster sizes (No UA). As far as the k_{fast} values were concerned, see Fig. 6, once the beginning of turbidity loss is reached, the particles or clusters seem to be settling faster in sonicated systems compared to the non-sonicated ones. In fact, in the last case, a larger population of cluster diameters (see Table 1)

indicates these will settle at different times and have therefore low k_{fast} values compared to those obtained with sonicated systems. Visual observation confirms that for no UAP conditions, the alumina concentration seems very different at the top of the cuvette compared to the bottom of it, while this concentration remained relatively constant at each height of the cuvette for UAP conditions. In this last case, this phenomenon resulted in a drastic change in the U vs. t plot when the diode threshold was reached. It must be pointed out that the k_{fast} value for a concentration of 100 $g.l^{-1}$ of alumina and for a sonicated system was not evaluated due to a lack of data.

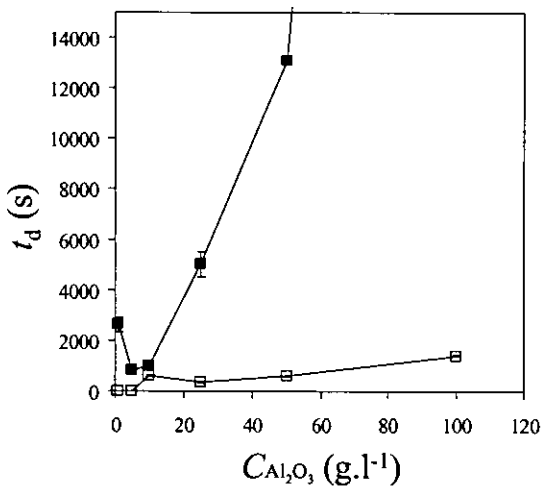

Fig. 5 – Destabilization time vs. γ-Al_2O_3 concentration in the bath (no surfactant); without (□) and with ultrasonic agitation prior to measurement (UAP) (■).

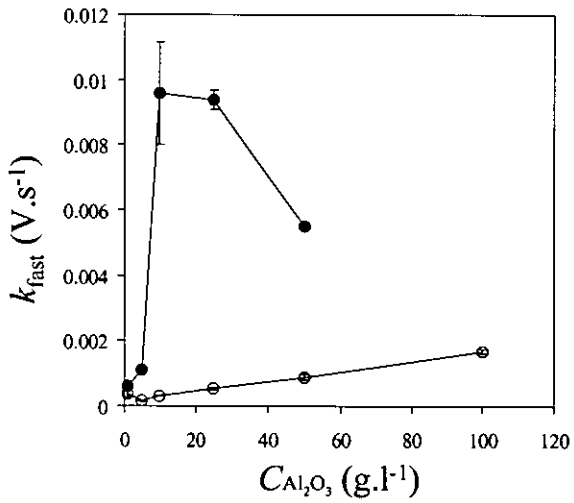

Fig. 6 - k_{fast} vs. γ-Al_2O_3 concentration in the bath (no surfactant); without (○) and with ultrasonic agitation prior to measurement (UAP) (●).

Electroplating and coating analysis

In the plating experiments assessing the impact of surfactant, CTAC-L conditions were chosen in order to use a minimum concentration of additive, to have the highest possible

zeta potential values and obtain the most dispersed alumina particle system. In terms of ultrasonic agitation, solutions were either sonicated 15 minutes prior to plating or sonication was applied before and during the plating experiments. Figures 7 to 10 show the SEM micro images of cross-sectioned Co-γ-Al_2O_3 coatings where the hydrodynamic conditions and the alumina concentration were the variables. For each of the chosen γ-Al_2O_3 concentrations (10, 20 and 25 $g.l^{-1}$), it was clearly visible that the sonicated systems (UAD) produced coatings with better particle dispersion compared to systems not sonicated during plating. In order to quantify the apparent cluster size versus the plating conditions, between 30 to 50 measurements were performed per SEM picture and all the data are reported in Table 2. The cluster size reduction was particularly spectacular for $C_{Al_2O_3}$ = 25 $g.l^{-1}$, see Fig. 10a, where cluster sizes up to 2 μm in diameter were observed under no sonication. It must be pointed out that since the measurement of a given cluster was performed in 2-D, its size may be even larger since only a slice of it is measured. In this table, the effect of UAD on cluster size was confirmed, where aggregate sizes varied between 301 and 505 nm for sonicated systems while they ranged between 726 and 1080 nm without sonication. It is also worth noticing that the average standard deviation for the cluster size for the non sonicated systems was higher compared to the sonicated ones: 67 % and 23.5 % respectively. In the non-sonicated plating systems, presence of CTAC did not lower cluster size at $C_{Al_2O_3}$ = 10 $g.l^{-1}$, while for the sonicated system the aggregate size was marginally reduced. This observation confirmed the results obtained with the turbidimetric measurements where ultrasonic agitation was the determining factor in lowering the cluster size. In this particular case, CTAC molecules do not act as dispersants, but rather as a surface active molecule tailoring the particles' surface charge

(change in zeta potential). Figures 7a, 8a, 9a and 10a show an important level of particle agglomeration, indicating that ultrasonic agitation must take place during the electroplating process in order to achieve fine particle dispersion. This re-agglomeration process probably also occurred during the zeta potential experiments where cluster sizes were respectively 3 μm and 3 to 4 μm when additive free and CTAC-L solutions were sonicated just prior to the measurements. Higher alumina concentrations seem particularly affected by the effect of ultrasonic agitation. In fact, a 25 $g.l^{-1}$ alumina concentration had cluster sizes that were on average 200 nm bigger than those produced by the 20 $g.l^{-1}$ alumina plating bath, within the same ultrasonic conditions. This can be explained by the fact that more ultrasonic power might be needed to disperse high alumina bath content.

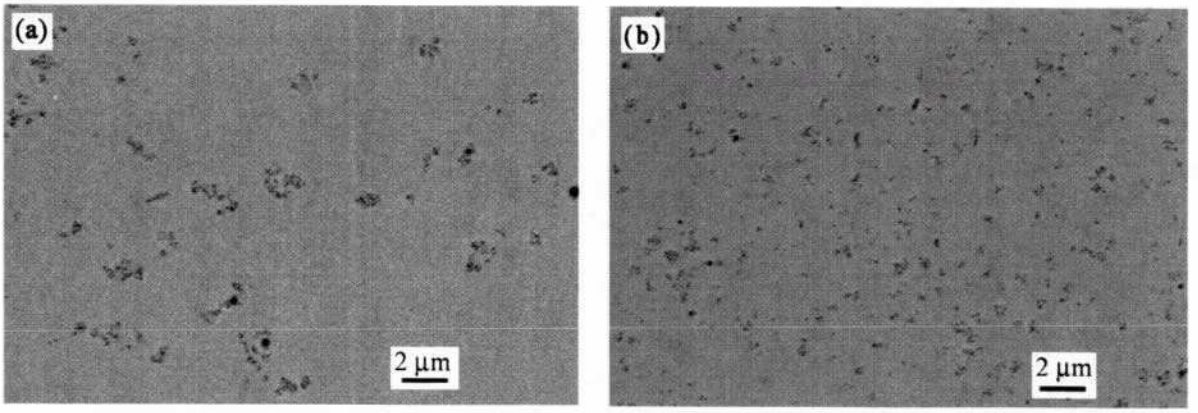

Fig. 7 – Co-γ-Al_2O_3 SEM cross-section micrograph. Plating conditions: No surfactant and $C_{Al_2O_3}$ = 10 $g.l^{-1}$.

(a) Ultrasonic agitation prior (UAP) and (b) during plating (UAD).

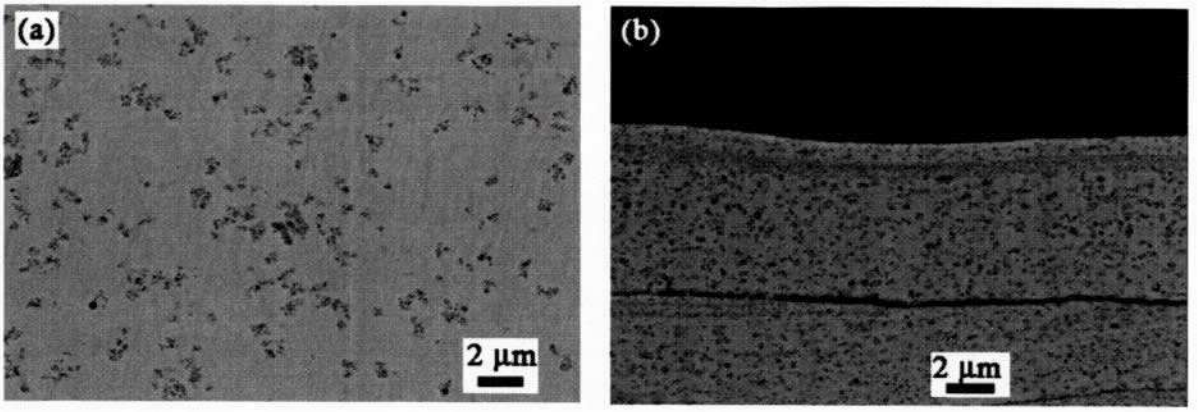

Fig. 8 – Co-γ-Al_2O_3 SEM cross-section micrograph. Plating conditions: CTAC-L and $C_{Al_2O_3}$ = 10 g.l^{-1}. (a) Ultrasonic agitation prior (UAP) and (b) during plating (UAD).

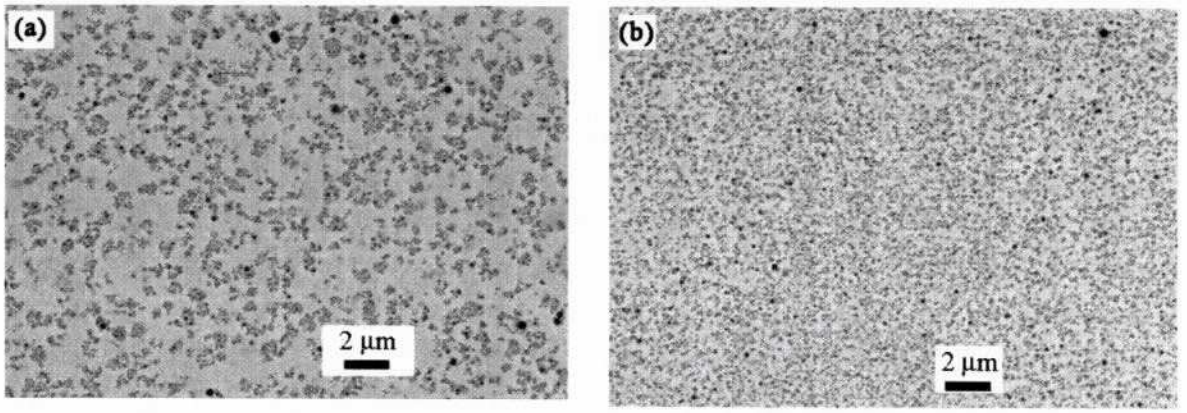

Fig. 9 – Co-γ-Al_2O_3 SEM cross-section micrograph. Plating conditions: CTAC-L and $C_{Al_2O_3}$ = 20 g.l^{-1}. (a) Ultrasonic agitation prior (UAP) and (b) during plating (UAD).

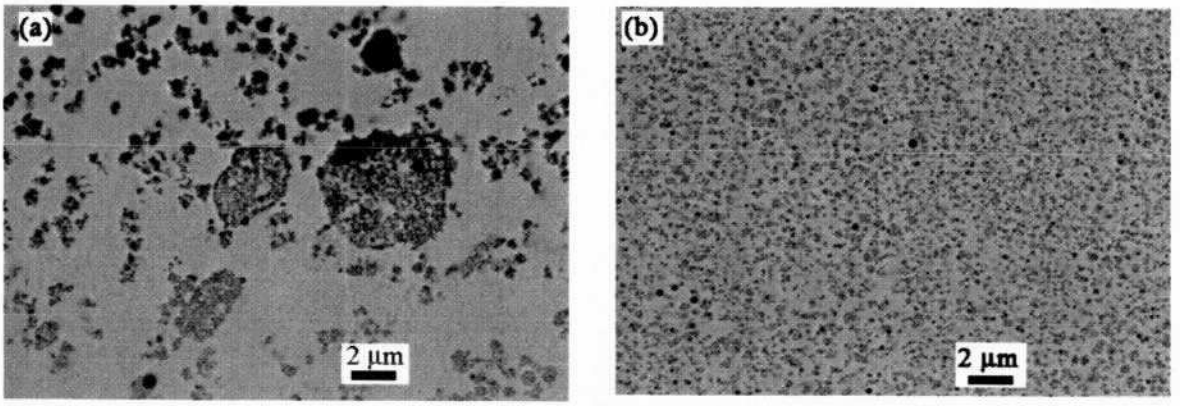

Fig. 10 – Co-γ-Al_2O_3 SEM cross-section micrograph. Plating conditions: CTAC-L and $C_{Al_2O_3}$ = 25 g.l^{-1}. (a) Ultrasonic agitation prior (UAP) and (b) during plating (UAD).

Table 2 – γ-Al_2O_3 cluster size inside the coating vs. plating conditions.

		UAP		UAD	
CAl_2O_3 ($g.l^{-1}$)	Surfactant	Cluster average size (nm)	Dev. (%)	Cluster average size (nm)	Dev. (%)
10	0	726	62	375	37
10	CTAC-L	908	106	361	23
20	CTAC-L	744	14	301	20
25	CTAC-L	1080	86	505	14

In order to investigate the influence of UA and the addition of CTAC upon particle inclusion percentage, the aluminum atomic percentage was evaluated using an EDX probe during SEM cross-sectional analysis. The corresponding data for two concentrations of alumina (10 and 20 $g.l^{-1}$) are displayed in Fig. 11. The influence of CTAC addition was very important, since without this molecule present in the plating bath, the aluminum content was close to 0.5 % and this independently of the hydrodynamic conditions. On the other hand, this value was raised by a factor of 50 (UAP) to 60 (UAD) when CTAC was added to the solution, supporting the importance of zeta potentials on particle inclusion in electrocomposite coatings. As far as the hydrodynamic conditions were concerned, for UAD and CTAC-L conditions, particle inclusion percentages were raised compared to UAP and CTAC-L conditions: + 1.61 % and + 1.44 % for CAl_2O_3 = 10 and 20 $g.l^{-1}$ respectively. For each hydrodynamic system, the inclusion percentage slightly increased (within the experimental error) with alumina concentration increase: + 0.27 % for UAP and + 0.09 % for UAD. These results show that the combined effects of ultrasonic agitation during plating (UAD) and CTAC addition to

the plating bath had positive effects on the enhancement of alumina particle inclusion into the cobalt matrix.

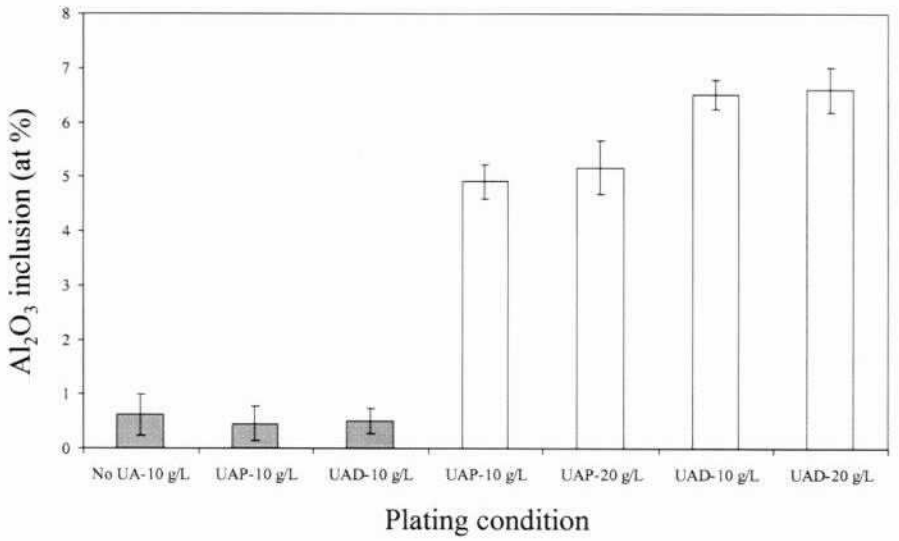

Fig. 11 – γ-Al_2O_3 percentage inclusion versus plating conditions at 10 or 20 g/L of alumina bath concentration. Grey bars: No surfactant and white bars: CTAC-L.

Figure 12 shows the Knoop hardness for the Co-γ-Al_2O_3 nanoelectrocomposite coatings obtained at different alumina bath concentrations. It is clearly visible that the inclusion of alumina particles increases the hardness of the cobalt by 150 HKN for baths containing 5 and 10 $g.l^{-1}$ of alumina particles and this independently of the agitation mode. This increase is in the 150 to 200 HKN range for baths containing 20 to 25 $g.l^{-1}$. However, for this last case, the measurements remained very close or within the experimental error. The effect of ultrasonic agitation during electroplating upon coating hardness is not significant. Although good particle dispersion and inclusion was obtained for the Co-γ-

Al_2O_3 system when UAD was used compared to UAP, no significant improvement in hardness was observed.

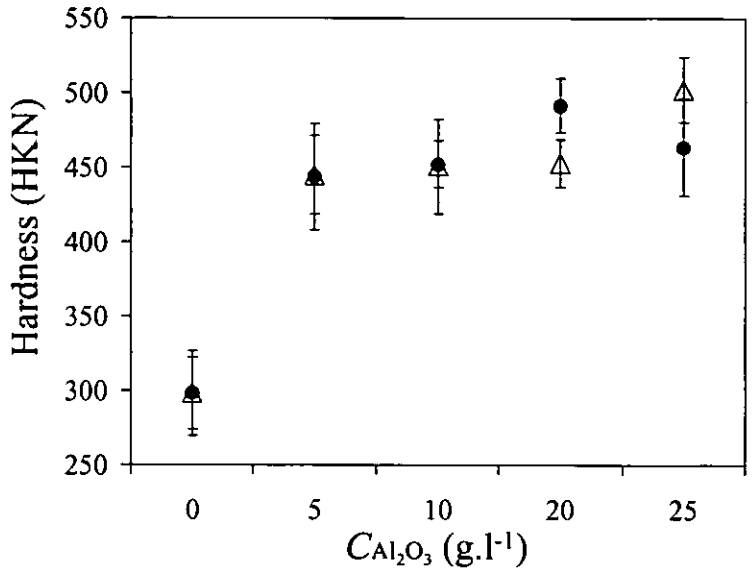

Fig. 12 – Cobalt and Co-γ-Al_2O_3 Knoop hardness values versus bath Al_2O_3 concentration. CTAC–L, ultrasonic agitation prior (△) and during electroplating (●).

Finally, it should be pointed out that some peeling was noticed on the coating surface when both ultrasonic agitation and CTAC were used. However, no peeling was observed (only slight pitting) when solutions were additive free. In fact, the surface active agent may have changed the grain structure of deposits and therefore their internal or residual stress that can lead to poor coating adhesion.

Conclusion

The effects of the cationic surfactant (CTAC) addition and ultrasonic agitation during plating of Co-γ-Al_2O_3 nanoelectrocomposite coatings resulted in high particle inclusion percentage with alumina aggregates being 2.5 to 3.0 times smaller than the conventional plating and when ultrasonic agitation was used only before plating. CTAC addition resulted in raising alumina particle zeta potentials and high inclusion percentages into the cobalt matrix. For its part, ultrasonic agitation during electroplating acted mainly as an alumina cluster refiner, while combination with surfactant showed synergistic effects. In order to improve particle dispersion and inclusion percentage as well as to reduce coating internal stress, future work will be focused towards the variation of plating current density, the cobalt ion concentration, the ultrasonic power and frequency as well as the choice (and concentration) of other cationic surfactants that can produce low stress deposits. Although good particle dispersion was obtained for the Co-γ-Al_2O_3 system deposited under ultrasonic agitation, no real improvement in term of hardness was observed. However, the positive synergistic effect of cationic surfactant addition and ultrasonic agitation was clearly demonstrated and can be applied to other types of electrocomposite plating solutions and therefore to other types of coating applications like, for instance, self-lubricating electrocomposites (MoS_2 particles).

Acknowledgements

The authors wish to warmly thank the following people of IMI/NRC: Mélanie Bolduc for the electroplating experiments, Michel Thibodeau and Jean-François Alarie for their technical contributions in SEM image analysis and hardness measurements, as well as Mario Lamontagne for setting up the turbidimetry apparatus. The authors wish also to thank Dr Farid Bensebaa of ICPET/NRC in Ottawa for his kind help for the zeta potential measurements.

List of Symbols

Symbol	Meaning	Unit
$\vec{v}$	Particle electrophoretic velocity	$m.s^{-1}$
$\vec{E}$	Electric field	$V.m^{-1}$
ξ	Zeta potential	mV
η	Electrolyte viscosity	$m^3.kg^{-1}$
ε_0	Absolute permittivity (8.854×10^{-12})	$F.m^{-1}$
ε_r	Relative permittivity (80)	--
f	Ultrasonic frequency	kHz
k_{fast}	Steepest slope for of $U = f(t)$ curves.	$V.s^{-1}$
q	Particle charge	C
r	Particle radius	m
t	Time	s
t_d	Destabilization time	s
U	Diode potential in turbidimetry experiments	V
μ	Electrophoretic mobility	$m^2.s^{-1}.V^{-1}$

References

1. X.M. Ding, N. Merk, Scripta Mater. 37 (5) (1997) 685.
2. L.Orlovskaja, N. Periene, M. Kurtinaitiene, G. Bikulčius, Surf. Coat. Tech. 105 (1998) 8.
3. L. Benea, P.L. Bonora, A. Borello, S. Martelli, Wear 249 (2002) 995.
4. A.F. Zimmerman, D.G. Clark, K.T. Aust, U. Erb, Mater. Lett. 52 (2002) 85
5. K. H. Hou, M.D. Ger, L.M. Wang, S.T. Ke, Wear. 253 (2002) 994
6. M.L. Klingenberg, E.W. Brooman, T.A. Nagy, Proceedings of the American Electroplaters and Surface Finishers SUR/FIN Conference, pp. 684-96. June 23-26, 2003, Milwaukee, WI, USA.
7. M. Musiani, Electrochim. Acta 45 (2000) 3397.
8. K. Helle, F. Walsh, T. I. Met. Finish. 75 (2) (1997) 53.
9. J.L. Stojak, J. Fransaer, J.B. Talbot in Advances in Electrochemical Science and Engineering, Ed: R.C. Alkire and D.M. Kolb, Vol. 7, Wiley-VCH, Weinheim, Germany, 2002, p. 193.
10. J.P. Celis, J.R. Roos, C. Buelens, J. Electrochem. Soc. 134 (1987) 1402.
11. J. Fransaer, J.P. Celis, J.R. Roos, J. Electrochem. Soc. 139 (1992) 413.
12. T.W. Tomaszewski, L.C. Tomaszewski, H. Brown, Plating 56 (1969) 1234.
13. O. Berkh, S. Eskin, J. Zahavi, Plat. Surf. Finish. 81(3) (1994) 62.
14. Y.M. Henuset, R. Menini, Plat. Surf. Finish. 89(9) (2002) 63.

15. K. Helle, A. Opschoor, Proceedings of the tenth World Congress on Metal Finishing, p. 234, Ed. S. Haruyama, Kyoto, Japan, October 12-17, (1980).

16. N. Periene, A. Cesuniene, L. Taicas, Plat. Surf. Finish. 80(10) (1993) 73.

17. L. Orlovskaja, N. Periene, M. Kurtinaitiene, S. Surviliene, Surf. Coat. Tech. 111 (1999) 234.

18. A. Grosjean, M. Rezrazi, M. Tachez, Surf. Coat. Tech. 96 (1997) 300.

19. B. Bozzini, G. Giovannelli, F. Ferrari, G. Arman, G. Bollini, L. Nobili, P.L. Cavallotti, Proceedings of the Interfinish'96 World Congress, p. 277, Birmingham, UK, September 10-12, (1996).

20. F. Erler, C. Jakob, H. Romanus, L. Spiess, B. Wielage, T. Lampke, S. Steinhäuser, Electrochim. Acta 48 (2003) 3063.

21. J.B. Talbot, Proceedings of the American Electroplaters and Surface Finishers SUR/FIN Conference, pp. 701-13. June 23-26, 2003, Milwaukee, WI, USA.

22. G.S. Petit, R.R. Wright, T. Kwasnoski, C.W. Weber, Plat. Surf. Finish. 64(10) (1977) 46.

23. W.-H. Lee, S.-C. Tang, K.-C. Chung, Surf. Coat. Tech. 120-121 (1999) 607.

24. J. Steinbach, H. Ferkel, Scripta Mater. 44 (2001) 1813.

25. A. Fan, P. Somasundaran, N.J. Turro, Langmuir 13 (1997) 506.

Captions to Figures

Fig. 1. Schematic representation of the electroplating set-up.

Fig. 2. Top view of the apparatus for turbidimetric measurements. (1) Quartz cuvette, (2) detector and (3) laser source.

Fig. 3. Zeta potential of γ-Al_2O_3 particles (C = 1 g.l^{-1}) in cobalt plating bath vs. surfactant type and concentration. (○) without (No UA) and (●) with ultrasonic agitation (UAP).

Fig. 4. Turbidimetric measurements: diode potential vs. time at 25 g.l^{-1} γ-Al_2O_3 concentration and no surfactant. Without (No UA) (A) and with ultrasonic agitation prior to measurement (UAP) (B).

Fig. 5. Destabilization time vs. γ-Al_2O_3 concentration in the bath (no surfactant); without (□) and with ultrasonic agitation prior to measurement (UAP) (■).

Fig. 6. k_{fast} vs. γ-Al_2O_3 concentration in the bath (no surfactant); without (○) and with ultrasonic agitation prior to measurement (UAP) (●).

Fig. 7. Co-γ-Al_2O_3 SEM cross-section micrograph. Plating conditions: No surfactant and $C_{Al_2O_3}$ = 10 g.l^{-1}. (a) Ultrasonic agitation prior (UAP) and (b) during plating (UAD).

Fig. 8. Co-γ-Al_2O_3 SEM cross-section micrograph. Plating conditions: CTAC-L and $C_{Al_2O_3}$ = 10 g.l^{-1}. (a) Ultrasonic agitation prior (UAP) and (b) during plating (UAD).

Fig. 9. Co-γ-Al_2O_3 SEM cross-section micrograph. Plating conditions: CTAC-L and $C_{Al_2O_3}$ = 20 g.l^{-1}. (a) Ultrasonic agitation prior (UAP) and (b) during plating (UAD).

Fig. 10. Co-γ-Al_2O_3 SEM cross-section micrograph. Plating conditions: CTAC-L and $C_{Al_2O_3}$ = 25 g.l^{-1}. (a) Ultrasonic agitation prior (UAP) and (b) during plating (UAD).

Fig. 11. γ-Al_2O_3 percentage inclusion versus plating conditions: CTAC-L and $C_{Al_2O_3}$ = 10 (white bars) and 20 g.l^{-1} (black bars).

Fig. 12. Cobalt and Co-γ-Al_2O_3 Knoop hardness values versus bath Al_2O_3 concentration. CTAC–L, ultrasonic agitation prior (△) and during electroplating (●).